Thermal transport in polyethylene and at polyethylene–diamond interfaces investigated using molecular dynamics simulation

2009 J. Phys.: Condens. Matter 21 084219

(http://iopscience.iop.org/0953-8984/21/8/084219)

IOP PUBLISHING JOURNAL OF PHYSICS: CONDENSED MATTER

J. Phys.: Condens. Matter **21** (2009) 084219 (8pp) doi:10.1088/0953-8984/21/8/084219

Thermal transport in polyethylene and at polyethylene–diamond interfaces investigated using molecular dynamics simulation

Boris Ni, Taku Watanabe[1] and Simon R Phillpot[2]

Department of Materials Science and Engineering, University of Florida, Gainesville, FL 32611, USA

E-mail: sphil@mse.ufl.edu

Received 18 July 2008, in final form 29 August 2008
Published 30 January 2009
Online at stacks.iop.org/JPhysCM/21/084219

Abstract

The thermal conductances across covalently bonded interfaces between oriented single crystal diamond and completely aligned polyethylene chains are determined for the three principal orientations of diamond. The calculated thermal conductances, which range over 690–930 MW m^{-2} K^{-1}, are consistent with those of other strongly bonded interfaces. These results suggest that the experimental interfacial conductances across hard–soft interfaces can be quite large if the bonding across the interface is strong, a conclusion that could have important implications for thermal management in bioelectromechanical systems and other inorganic–organic structures. The effects of defects and cross-linking on the thermal conductivity of polyethylene are also analyzed.

1. Introduction

While most nanostructures investigated to-date have been fabricated from purely inorganic materials, the study of organic/inorganic and bio/inorganic hybrid nanostructures is an important research frontier with enormous potential applications in areas such as bioMEMs and microelectronics. A key maintenance task in all nanostructures is to efficiently move this heat away from the active components into heat-management structures such that the functionality and structural integrity of the nanostructure are not compromised [1–3]. Indeed, there is a growing recognition that in many cases heat-management structures have to be designed into devices with the same care that is given to the design of the primary functionality. The issue of thermal management in organic/inorganic systems is potentially even more critical since the very structure of many organic materials can be irreversibly compromised by even rather modest temperatures increases.

Because of the wide range of electronic applications, many recent studies of heat flow at organic/inorganic interfaces relate to polymer/metal joints. The range of values determined for the interfacial conductance is extremely wide. Marotta *et al* [4] measured the thermal contact conductance between Al and several commercially important thermoplastic and thermosetting polymers. Of all of the systems that they studied, the largest interfacial conductance was found for a polyethylene/Al joint with values in the range ∼1.1–1.7 kW m^{-2} K^{-1}. Analogous experiments were carried out by Fuller *et al* [5] on thermal joints of four different polymers with aluminum yielding interfacial conductances ranging from ∼40 to 250 W m^{-2} K^{-1}. Mirmira *et al* [6] found the interface conductance of GTA Grafoil with Al to be ∼32 kW m^{-2} K^{-1}. Finally, a recent determination of the Kapitza resistance between a polymer, polymethyl methacrylate (PMMA), and alumina yielded a value of $G \sim 30 \pm 10$ MW m^{-2} K^{-1} near room temperature [7]. Considerably higher values (100 MW m^{-2} K^{-1} and above) have been determined for the interfacial conductance in purely inorganic systems [2, 8–14].

In this paper, we address the question as to how high could the interfacial conductance of an organic/inorganic interface be under optimum conditions. To address

[1] Present Address: School of Chemical and Biomolecular Engineering, Georgia Institute of Technology, Atlanta, GA 30332, USA.

[2] Author to whom any correspondence should be addressed.

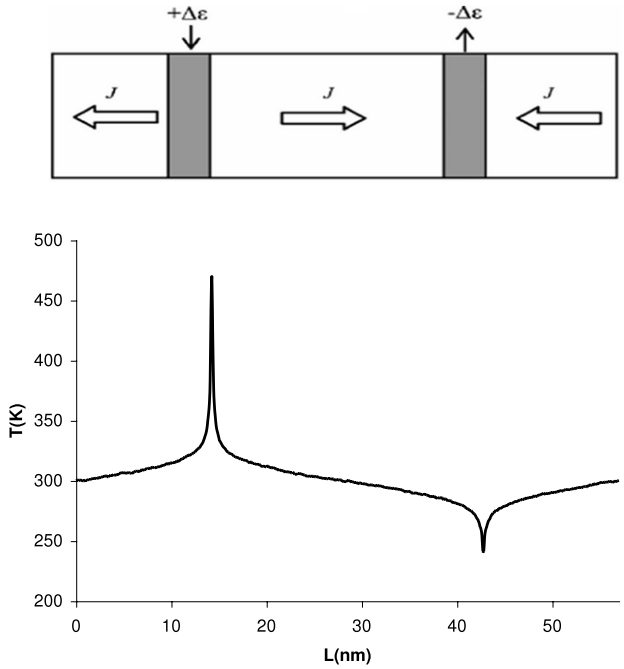

Figure 1. (a) The location of the heat source and heat sink one-quarter and three-quarters of the way along the simulations cell ensures identical heat fluxes through the center of the cell and through the periodic boundary. (b) The steady-state temperature profile in diamond at 300 K for a simulation cell of 160 unit cells length; the spikes correspond to the locations of the heat source and the heat sink.

this question, we use atomic-level simulation methods to explore the thermal transport properties across highly idealized polyethylene/diamond interfaces, which we take as a prototypical organic/inorganic system. We find that, in principle organic/inorganic interfaces should be able to conduct heat as well as inorganic/inorganic interfaces if there is strong bonding at the interface itself.

2. Simulation Methodology

Molecular dynamics (MD) is the method of choice for the simulation of heat transfer processes at the atomic scale. To analyze the polyethylene/diamond system, we require some level of understanding of thermal transport in polyethylene (PE) and diamond separately. The reactive empirical bond order (REBO) potential can describe both diamond and polymeric systems [15, 16]. While it was originally designed for simulation of the reactive dynamics of hydrocarbons, the REBO potential has also been successfully applied to diamond, ion beam deposition, thin film growth, and properties of carbon nanotubes. For this study we use the second-generation REBO potential [16].

In computing the thermal conductivity we use the direct method, described in detail previously [17, 18]. Briefly, a heat current is established by adding and removing equal amounts of energy at the 'heat source' and 'heat sink' regions of the system. To produce a heat source and heat sink in the bulk of material we employ the velocity-rescaling mechanism of Jund and Jullien [19]. Figure 1(a) illustrates the computational setup. For a bulk system such as polyethylene or diamond, the thermal conductivity, k, can be determined from Fourier's law which can be written in scalar form as

$$J = -k\,\mathrm{d}T/\mathrm{d}z, \tag{1}$$

where J is the heat current along the z direction and $\mathrm{d}T/\mathrm{d}z$ is the temperature gradient.

For a system with an interface, the interfacial (Kapitza) conductance, G_K, is defined as

$$J = G_\mathrm{K}\Delta T, \tag{2}$$

where ΔT is temperature discontinuity at the interface.

The simulation cell is periodic in all three spatial directions. The location of the heat source and heat sink one-fourth and three-fourths of the way along the simulation cell ensures that there are identical heat currents from the source to the sink in both the $+z$ and $-z$ directions.

3. Thermal conductivity of diamond and polyethylene

Before analyzing the diamond–polyethylene interface, it is necessary to characterize the thermal transport properties of diamond and polyethylene separately.

3.1. A thermal conductivity of diamond

The thermal conductivity of diamond has been determined previously by MD simulation [17, 20–22]. In those simulations the interatomic interactions were described by the Tersoff [23] and REBO [15, 16] potentials. Schelling *et al* [17] predicted the thermal conductivity of diamond described by the Tersoff potential to be 573 ± 60 W m^{-1} K^{-1} at 1000 K using the direct method. Che *et al* [20] obtained a value of ∼1200 ± 200 W m^{-1} K^{-1} for the REBO potential at 300 K using the Green–Kubo method. This is much lower than the estimate of the Rosenblum *et al* of ∼3220 W m^{-1} K^{-1} for the REBO potential at 300 K, however using the phonon spectrum method [21]. In this study we use the direct method because it is also well suited to compute interfacial Kapitza conductance [17].

Figure 1(b) shows the temperature profile determined using the REBO potential, obtained from a simulation of 2 million steps with a time step of 0.2 fs. Consistent with the results of earlier simulations [17], the temperature gradient is set within 200 000 steps. We therefore averaged the temperature profiles over the last 1.8 million steps.

As discussed in detail elsewhere, the thermal conductivity determined from simulation of diamond [17, 20], and other materials [24, 25] depends strongly on the simulation cell size. We have therefore determined the thermal conductivity for four different system sizes: 8 × 8 × 40, 8 × 8 × 80, 8 × 8 × 160 and 8 × 8 × 320 diamond unit cells. Following the previous analysis [17, 22, 24, 25], we expect the inverse of the thermal conductivity to be proportional to the inverse of the system size, as figure 2 shows is indeed the case. From

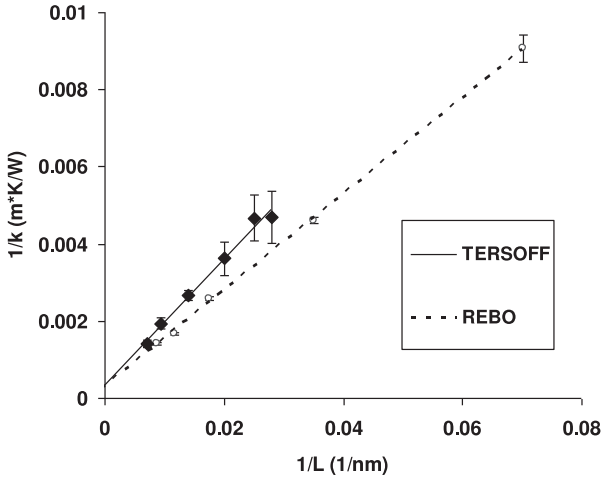

Figure 2. The linear relationship between the inverse thermal conductivity and the inverse length of the simulation cell length allows the thermal conductivity of diamond, as described by the REBO and Tersoff potentials, to be accurately estimated by extrapolation.

the extrapolation of this plot to infinite system size ($1/L = 0$), we estimate a room-temperature bulk thermal conductivity of 3300 ± 700 W m^{-1} K^{-1}. In the same figure we also show the previously determined size dependence obtained using the Tersoff potential [23]; this potential predicts a bulk thermal conductivity of (2740 ± 70) W m^{-1} K^{-1}. Interestingly our estimate for the thermal conductivity is essentially identical to that obtained using the phonon spectrum method; the agreement between these two results suggests that the true REBO estimate for the thermal conductivity of diamond is 3200–3300 W m^{-1} K^{-1}. Although natural diamond has a thermal conductivity of $\sim$2200 W m^{-1} K^{-1} [26], it is very interesting to note that nearly pure (containing 0.07% of C^{13}) has been found experimentally to have a thermal conductivity of $\sim$3300 W m^{-1} K^{-1} [27, 28], which is extremely well matched by the REBO calculations.

3.2. Thermal conductivity of polyethylene

Given that the REBO potential seems to predict the thermal conductivity of diamond very well, it is with some confidence that we can use it to characterize the thermal transport properties of polyethylene.

Experimentally, polymers generally have low thermal conductivities, κ typically being 1 W m^{-1} K^{-1} or less. This low thermal conductivity largely arises from their complex morphologies. While many polymers are amorphous, even semicrystalline polymers contain significant amounts of amorphous material; for example, semicrystalline polyethylene consists of spherulites of largely crystalline lamellae, which either impinge on each other directly or are separated by an amorphous matrix. This morphology can often be quite easily manipulated. For example, while the thermal conductivity is isotropic in an unoriented polymer, it can be strongly anisotropic in an oriented polymer [29]. Pietralla showed that the thermal diffusivity, α ($\kappa = \rho C_p \alpha$, where C_p is the specific heat at constant pressure and ρ the density) of polyethylene is a strong function of the draw ratio, i.e., by how much the polymer is uniaxially stretched, thereby increasing the alignment of the polymer chains [30]. This indicates that the intrinsic thermal conductivity along the polymer chains is quite high; this led Pietralla to estimate that thermal conductivities of up to 70 W m^{-1} K^{-1} might be achievable for polyethylene with the properties of a single chain [30]. Since we are interested in the conceptual limit in the performance of these materials,

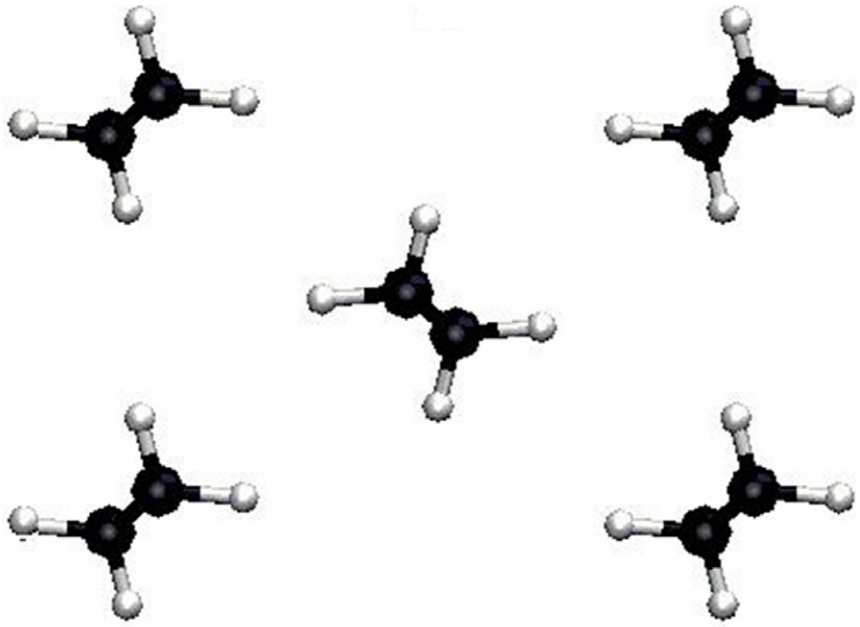

Figure 3. End-on view of the orthorhombic unit cell of crystalline polyethylene, which contains two chains in the areal unit cell.

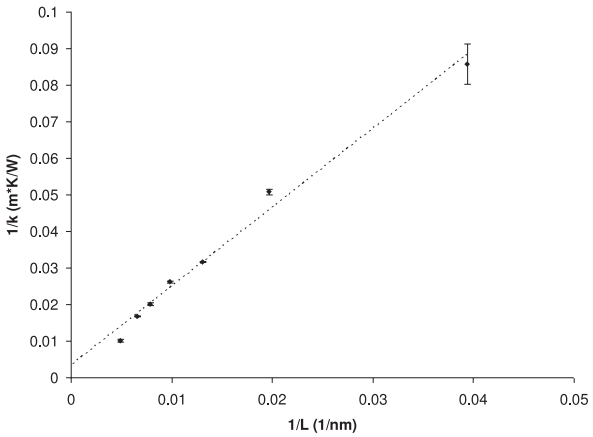

Figure 4. The linear relationship between the inverse thermal conductivity and the inverse length of the simulation cell length allows the thermal conductivity of polyethylene to be accurately estimated by extrapolation.

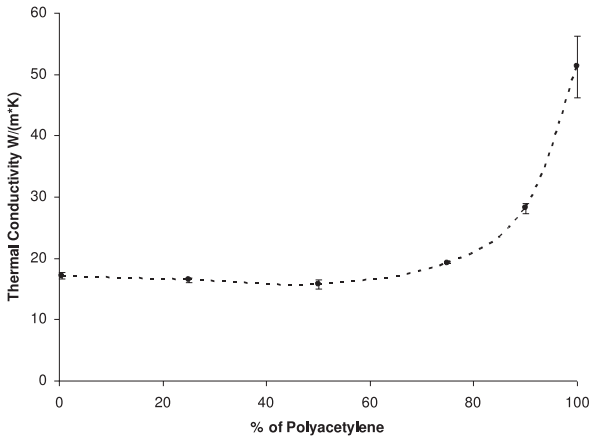

Figure 5. The thermal conductivity of polyethylene–polyacetylene random copolymers as a function of the percentage of polyacetylene.

we consider this limit of fully aligned chains. To do this, we simulate completely crystalline PE, see figure 3 [31, 32].

Following the same computational procedure as for diamond, we calculate the thermal conductivity of crystalline PE along the polymer chains for different sizes of simulation cell. Each simulation cell is 4 unit cells by 6 unit cells in the directions normal to the chain direction. Along the chain directions, we consider $N = 100$, 200, 300, 400, 500, 600 and 800 unit cells, corresponding to chains with molecular weights of 2.8×10^3, 5.6×10^3, 8.4×10^3, 1.12×10^4, 1.4×10^4, 1.68×10^4 and 2.24×10^4. We average the temperature profile after 300 000 MD steps with 0.1 fs time step. The time step for these PE simulations is smaller than for diamond because of the presence of high-frequency vibrational modes in PE that are absent in diamond. The calculated thermal conductivities increase monotonically from 11.7 to 99.6 W m^{-1} K^{-1} as the length of the polymer chains increases.

We can interpret the limit of infinite system size as corresponding to an infinite molecular weight, for which the thermal conductivity should reach its highest possible value. Again a $1/k$ versus $1/L$ plot (figure 4) yields the expected linear fit. Making a linear extrapolation we obtained the axial thermal conductivity of a PE crystal of infinite molecular weight to be 310 ± 190 W m^{-1} K^{-1}. This is considerably larger than either the extrapolated value of 70 W m^{-1} K^{-1} given by Pietralla [30] or the value of $\sim$40 W m^{-1} K^{-1} experimentally determined by Choy *et al* for ultradrawn single crystal PE mats with molecular weight 5.2×10^6 and draw ratio $\lambda = 350$, and for gel PE at 295 K [33].

One of the reasons for the discrepancy between our calculated values and the experimental values is probably the absence of imperfections in the simulated PE structure. Given that even crystalline polymers never have a perfect defect-free crystal structure, it is interesting to study how different kinds of defects and impurities impact the calculated thermal conductivity of PE. One simple kind of defect arises from the presence of unsaturated carbon atoms and the concomitant reduction in the number of hydrogen atoms along the aliphatic chains. In a real system this leads to sp^2 hybridization in these regions and the presence of double bonds. The corresponding effect within the REBO potential is the reduction of C–C bond lengths to values corresponding to C=C bonds. We have systematically varied the percentage of C=C double bonds from 0% to 100% thus spanning the range from pure PE (0%) to a poly (ethylene–acetylene) mixture (50%) and finally to pure polyacetylene (PA)(100%). The structure of PA is taken from the literature [34, 35].

Figure 5 shows the dependence of axial thermal conductivity on the fraction of PA for chains containing 400 C atoms, which corresponds to molecular weights of 5.6×10^3 for PE and 5.2×10^3 for PA. We see that the thermal conductivity of PE is considerably less than that of PA. This is quite reasonable since the C=C double bonds in PA are shorter than those in PE, thus increasing the efficiency of heat transport. Moreover, the C atoms in PA have only one C–H bond rather than two as in PE. Thus there are fewer energy-dissipating vibrations associated with the H side groups in PA than in PE.

This difference in the intrinsic thermal transport properties of PE and PA also explains the composition dependence of the thermal conductivity seen in figure 5. We expect that the presence of any kind of defect will tend to reduce the thermal conductivity. However, the PA segments added to the PE have a higher intrinsic thermal conductivity than the PE itself. Evidently from figure 5 the decrease due to the presence of the PA defects is almost exactly balanced by the increase in the thermal conductivity due to the superior intrinsic thermal transport properties of the PA segments themselves. When PE defects are added to PA, the presence of the defects themselves and their lower intrinsic thermal conductivity lead to a strong decrease in the overall thermal conductivity. There are some experimental results on the thermal transport properties of polymer blends [36–38] which are broadly consistent with what we see in simulation. However, these are qualitatively different systems from the PE/PA copolymers considered here. In a blend the thermal properties of the constituents are not changed; as a result the thermal transport can be understood in terms of a rule of mixtures. By contrast in the PE/PA copolymer, the vibrational modes themselves and

Table 1. Structural measures and interfacial thermal transport properties of diamond/PE interfaces for (001), (011) and (111) oriented diamond.

Diamond surface	(001)	(011)	(111)
Diamond unit cell (Å)	7.112/14.224	14.224/10.579	12.318/10.058
PE unit cell (Å)	7.388/14.787	14.776/9.858	14.776/9.858
Mismatch (%)	$+3.1/+3.8$	$+3.7/-6.8$	$+20.0/-2.0$
Diamond/PE length (unit cells)	70/100	50/100	30/100
Simulation cell length (Å)	1005.6	1010.7	1031.0
Diamond/PE bonds	6	8	8
Interfacial bond density ($Å^{-2}$)	0.059	0.053	0.064
ΔT (K)	51.2 ± 6.1	40.5 ± 2.9	34.8 ± 6.2
G_k (MW m^{-2} K^{-1})	770 ± 100	690 ± 50	930 ± 140

their interactions with each other, which determine the thermal transport properties, change with composition.

Another type of defect that could significantly alter the thermal conductivity in polymers is cross-linking. We calculate the thermal conductivity of PE with 5% and 10% of the C atoms on each chain being cross-linked; these result in 26.6% and 44.2% reductions in the thermal conductivity, respectively. A possible reason for this dependence is that the distances between cross-links along the chains, ∼101 Å and ∼51 Å apart for 5% and 10% cross-linking respectively, comparable to the average phonon mean free path in pure PE, which we estimate from the usual kinetic formula to be ∼54 Å.

3.3. Interfacial conductance of diamond–polyethylene interfaces

Interfaces become a major factor in the thermal transport properties of structures and devices when the system size approaches the scale of mean free path of heat-carrying phonons, which is typically ∼100 nm or less. Experiment demonstrates that the interfacial conductance has dramatic effect on effective thermal conductivity in thin films and composite materials [10–14].

There are a large number of different choices that can be made for the morphology of the PE/diamond interface. On the diamond side, we look at the three principal surfaces: (001), (011) and (111). On the polyethylene side, we use pure un-crosslinked chains. This extremely idealized system should display the highest thermal interfacial conductance of any that we might construct, thereby establishing the upper bound on the interface conductance that we want to define. Here, we connect the polymer chains to the diamond surface with covalent bonds. It is physically reasonable that such strong bonds will lead to optimal interfacial thermal transport. Indeed, Dong *et al* [39] showed that chemical functionalization of micro-sized alumina particles fillers in a polymer composite material leads to an increase of effective thermal conductivity. The weak-bonding limit is defined by the polymer and diamond being coupled only through non-bonded interactions, for which case thermal transport across the interface should be extremely inefficient [40]. Thus we can expect that the interfacial conductance will be dominated by the strong covalent bonds if they are present in any significant density.

Figure 6(a) shows the initial interface structures, constructed based purely on the crystallography of the systems. In each case, we choose the structure so that the commensurability between the in-plane unit cells of the diamond and the polyethylene is maximized; the unit cell dimensions are given in table 1. For the case of the (111) surface, it is necessary to compress the polyethylene in one direction by 20%. However, even such a large compression should not significantly affect the thermal conductivity along the PE chains because of the weak inter-chain van der Waals interactions. So as to minimize any possible differences in the effects of system sizes, all the PE/diamond systems are constructed to have approximately the same length (see table 1). To set up the initial structure, we orient the polyethylene chains perpendicular to the interface boundary and adjust the atom positions somewhat to maximize the number of covalent bonds between across the interfaces. It can be seen in figure 6(a) that the (011) and (111) terminated diamond surfaces provide very dense bonding to polyethylene, with all of the end carbon atoms of polymer chains being positioned conveniently close to the surface. By contrast, the (001) surface does not provide such a good match in atomic positions across the interface: of the six polyethylene chains, only two could be simultaneously positioned close to two (001) diamond surfaces, with the remaining four not being covalently bonded.

Prior to the simulation of the thermal transport properties, we carefully equilibrated the PE/diamond structures. Figure 6(b) shows the structures of the interfaces after the system has been allowed to equilibrate. It is evident that in each case there is significant local structural rearrangement at the interface. In particular, for the (001) diamond case all of polymer chains manage to bond covalently to diamond surface. This is made possible by the fact that the (001) diamond surface has two dangling bonds. Indeed, we observe not only bonding of (001) diamond to PE but also the transfer of a few hydrogen atoms from the PE to diamond surface. The resulting undercoordinated carbon atoms in the PE bond to two carbons of diamond surface thus strengthening the bonding of the materials. We perform the thermal conductivity calculations on these well-bonded interfaces.

Figure 7(a) shows a typical computational setup for the simulation of the thermal conductivity. The system is constructed with two identical diamond crystals separated by two identical PE crystals. The heat source and sink are placed in the center of the diamond crystals. Thus this system contains four morphologically identical diamond/PE interfaces.

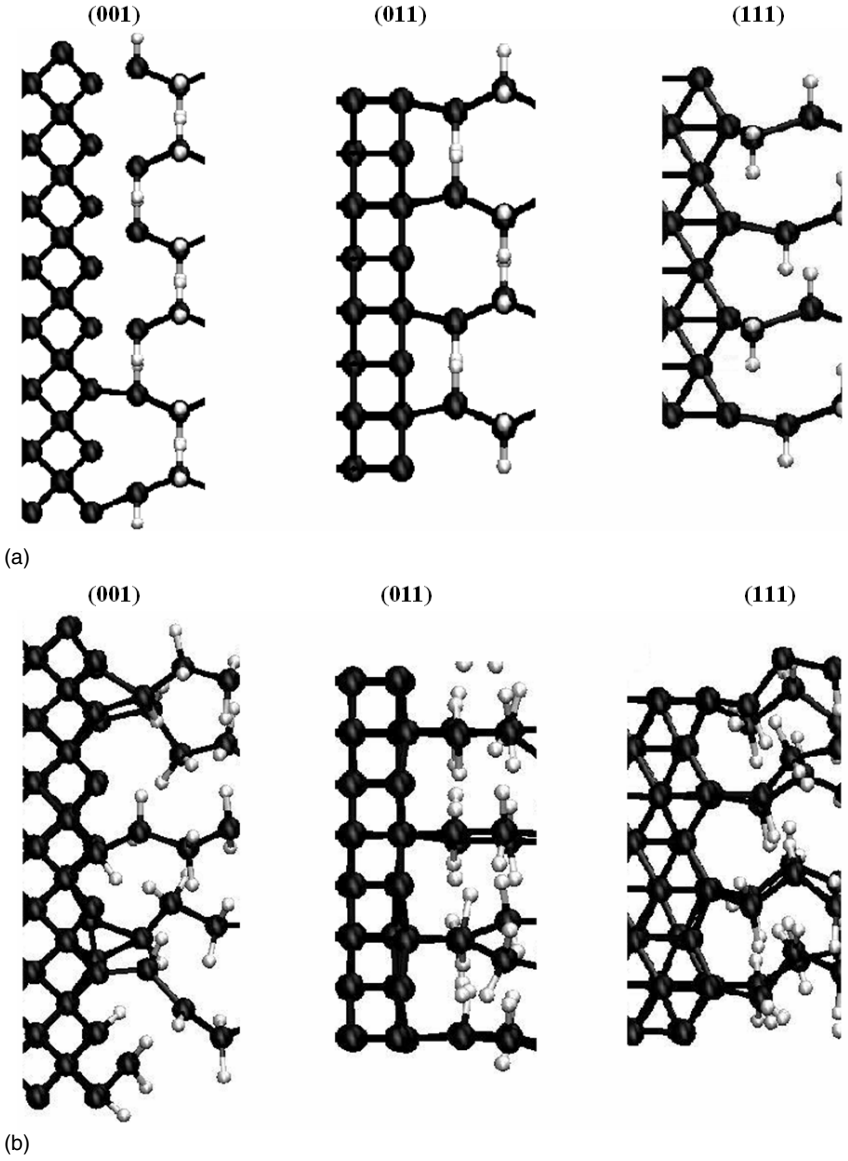

Figure 6. (a) Initial structure of the polyethylene/diamond interface constructed purely from crystallography. (b) The corresponding structures after the interfaces have been annealed at room temperature show improved interfacial bonding, particularly for (001) diamond.

Since polyethylene is a much more dynamic system than diamond, one could expect a substantially longer temperature equilibration period. To accelerate the process of reaching steady state, we divide the system into thin slices and apply separate thermostats in each slice for the first 50 000 steps set to 300 K. The thermostats are then turned off and the heat source is turned on. We run each simulation for a total 2 million steps to ensure that the system reached steady state; the temperature profile is determined by averaging over the last five hundred thousands steps.

The measured temperature drops at the interfaces are shown in table 1 for $J = 1.29 \times 10^{11}$ J m^{-2} s^{-1}. The error bars in the values come from the scatter in the temperature drop among the four crystallographically identical interfaces. The corresponding interfacial conductances determined from equation (2) are $G_K = 930 \pm 140$ MW m^{-2} K^{-1} for (111)-oriented diamond, $G_K = 690 \pm 50$ MW m^{-2} K^{-1} for (011)-oriented diamond and $G_K = 770 \pm 100$ MW m^{-2} K^{-1} for (001)-oriented diamond.

The order in interface conductances: $G_k(111) > G_k(001) > G_k$ (011) can be rationalized as shown in table 1 on the basis of the bond density across the interface, with the orientation with the highest bond density, (111), showing the highest conductance and the orientation with the lowest bond density, (011), showing the lowest conductance.

Figure 8 shows the relationship between the interface conductance and the interface bond density. The line is not an unrestricted best linear fit through the data, but is constrained to go through the origin, justified by the physically reasonable expectation that the interfacial conductance is zero for zero interfacial bond density. Actually of course, there would be a small interfacial conductance even for this case, since there will still be van der Waals interactions between the diamond and the PE.

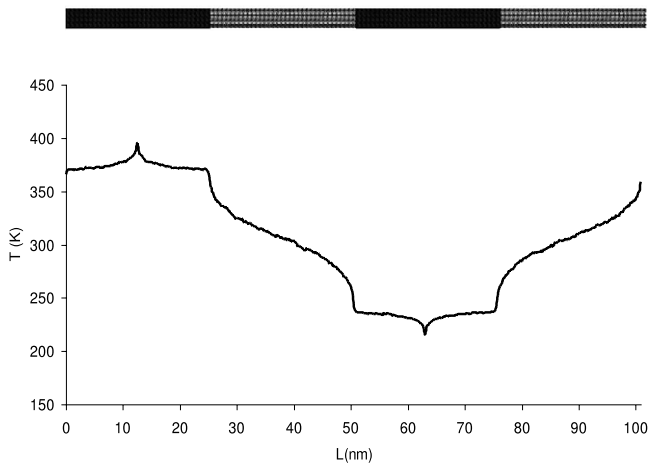

Figure 7. (a) Simulation cell for the interfacial conductance simulations. Diamond regions (dark) alternate with polyethylene regions (light). The heat source and sink are at the centers of the diamond regions. (b) Temperature profile through the polyethylene/diamond multilayer shows the temperature drops at the four crystallographically identical interfaces.

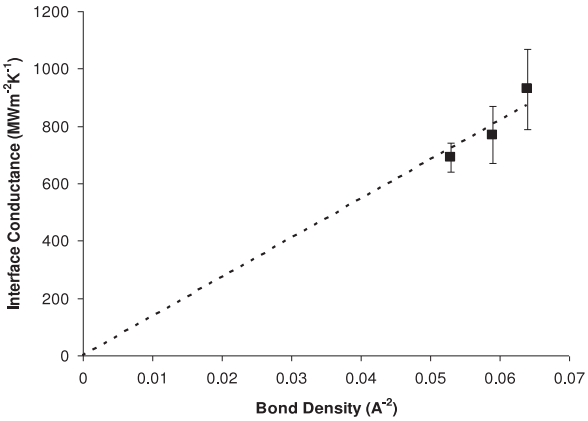

Figure 8. The interfacial conductance increases with increasing bond density at the interface. The dotted line is a linear fit through the origin.

We have also examined the dependence of the interfacial thermal conductance on the size of simulation cell. In particular, for the (011)-oriented diamond, we calculate the Kapitza conductance for a system that was twice as long as the original system, i.e., 100 unit cells in diamond crystals and 200 unit cells in each PE crystal; the overall system length is 2021.4 Å. We find that interfacial conductance for the larger system increases by 26% to 870 MW m^{-2} K^{-1}; we have previously seen a similar size dependence of grain boundaries in diamond [22], which was explained in terms of the restriction of the phonon mean free path by the length of simulation sample. Although there is a size dependence, there is no reason to expect that the size dependence will be different for the three different interfaces.

The calculated values for the PE/diamond interfacial conductance are large, though not without precedent. As discussed in the introduction, strongly bonded inorganic interfaces give interfacial conductances that reach values of hundreds of MW m^{-2} K^{-1}. Also, from the earlier MD simulations, the interfacial conductance in diamond was predicted to be 9–17 GW m^{-2} K^{-1} depending on the type of grain boundary [22]. Moreover, a simulation of a model diamond nanocrystal containing a number of high-angle (001) grain boundaries yielded an average interfacial conductance of ∼4.5 GW m^{-2} K^{-1} [9], a result that was reasonably consistent with the experimentally derived value ∼3 GW m^{-2} K^{-1} for ultrananocrystalline diamond thin films [9].

Our calculated values for the PE/diamond Kapitza conductance are an order of magnitude larger than the room-temperature values of 30–100 MW m^{-2} K^{-1} obtained at the interfaces between diamond and various metals such as Pb, Au, Al and Ti at room temperature [8]. The above experiments are also rather consistent with the values of 12–25 MW m^{-2} K^{-1} obtained by Huxtable *et al* [40] for interfacial conductance for non-covalently bonded systems. Thus, the large values of interfacial conductance are attributable to the covalent bonding between these materials. Similarly, in solid–liquid systems it was found that the interfacial conductance for a wetting interface is an order of magnitude higher than for the corresponding non-wetting interface [41].

4. Conclusions and outlook

Our simulations demonstrate the possibility of extremely high thermal transport in polyethylene and across polyethylene/diamond interfaces. The chemical purity and structural perfection of the polymer and the covalent bonding between these materials are the most important factors in improving their effective thermal conductivity. While we have explored the upper limit in the interfacial conductance of this organic/inorganic system, we have not addressed the issue as to whether it is experimentally possible to actually produce such well-bonded interfaces. Dehydrogenation of diamond surfaces can be obtained by annealing at 600–700 °C [42]. Moreover, the association of unsaturated alkenes (such as polyacetylene) to diamond occurs with little or no barrier as evidenced by experimental and theoretical investigation of cyclopentene chemisorption on (001) diamond [43]. In particular, Komatsu *et al* [44] demonstrated the possibility of chemically bonding ethane to (111) diamond. One can easily imagine an analogous reaction of chemisorption of an other alkane molecules onto diamond. Adhesion of adsorbates to the diamond surface can be dramatically increased [45] by surface dehydrogenation and creation of reactive sites such as C· radicals, polar C=O and π-bonded C=C groups. Thus PE bonding to the diamond is viable but may require additional chemical treatment. It may thus be anticipated that the increasing ability to functionalize surfaces may lead to methods for the systematic development of inorganic/organic interfaces with conductances similar to those of interfaces between inorganic materials.

Acknowledgments

We are happy to acknowledge the assistance of Hunter Henderson with some of the simulations. We are also happy to acknowledge a grant of computer time from the High

Performance Computing Center at the University of Florida. The work of BN was supported by a Grant from the Petroleum Research Fund of the American Chemical Society. The work of TW and SRP was supported by DOE-NERI Award DE-FC07-05ID14649

References

[1] Chen G 2006 *IEEE Trans. Compon. Packag. Technol.* **29** 238
[2] Cahill D G, Ford W K, Goodson K E, Mahan G D, Majumdar A, Maris H J, Merlin R and Phillpot S R 2003 *J. Appl. Phys.* **93** 793
[3] Goodson K E and Ju Y S 1999 *Annu. Rev. Mater. Sci.* **29** 261
[4] Marotta E E and Fletcher L S 1996 *J. Thermophys. Heat Transfer* **10** 334
[5] Fuller J J and Marotta E E 2001 *J. Thermophys. Heat Transfer* **15** 228
[6] Mirmira S R, Marotta E and Fletcher L S 1998 *J. Thermophys.* **12** 454
[7] Putnam S A, Cahill D G, Ash B J and Schadler L S 2003 *J. Appl. Phys.* **94** 6785
[8] Stoner R J and Maris H J 1993 *Phys. Rev.* B **48** 16373
[9] Angadi M A, Watanabe T, Bodapati A, Xiao X, Auciello O, Carlisle J A, Eastman J A, Keblinski P, Schelling P K and Phillpot S R 2006 *J. Appl. Phys.* **99** 114301
[10] Hasselman D P H, Donaldson K Y, Liu J, Gauckler L J and Ownby P D 1994 *J. Am. Ceram. Soc.* **77** 1757
[11] Hasselman D P H, Donaldson K Y, Thomas J R Jr and Brennan J J 1996 *J. Am. Ceram. Soc.* **79** 742
[12] Liu D M and Tuan W H 1996 *Acta Mater.* **44** 813
[13] Nan C W, Birringer R, Clarke D R and Gleiter H 1997 *J. Appl. Phys.* **81** 6692
[14] Nan C W, Li X P and Birringer R 2000 *J. Am. Ceram. Soc.* **83** 848
[15] Brenner D W 1990 *Phys. Rev.* B **42** 9458
[16] Brenner D W, Shenderova O A, Harrison J A, Stuart S J, Ni B and Sinnott S B 2002 *J. Phys.: Condens. Matter* **14** 783
[17] Schelling P K, Phillpot S R and Keblinski P 2002 *Phys. Rev.* B **65** 144306
[18] Schelling P K, Phillpot S R and Keblinski P 2004 *J. Appl. Phys.* **95** 6082
[19] Jund P and Jullien R 1999 *Phys. Rev.* B **59** 13707
[20] Che J, Cagin T, Deng W and Goddard W A III 2000 *J. Chem. Phys.* **113** 6888
[21] Rosenblum I, Adler J and Brandon S 1998 *Comput. Mater. Sci.* **12** 9
[22] Watanabe T, Ni B, Phillpot S R, Shelling P K and Keblinski P 2007 *J. Appl. Phys.* **102** 63503
[23] Tersoff J 1989 *Phys. Rev.* B **39** 5566
[24] Poetzsch R H H and Bottger H 1994 *Phys. Rev.* B **50** 15757
[25] Oligschler C and Schon J C 1999 *Phys. Rev.* B **59** 4125
[26] Lide D R 2005 *CRC Handbook of Chemistry and Physics* 86th edn (Boca Raton, FL: CRC Press)
[27] Anthony T R, Banholzer W F and Fleischer J F 1990 *Phys. Rev.* B **42** 1104
[28] Olson J R, Pohl R O, Vandersande J W, Zoltan A, Anthony T R and Banholzer W F 1993 *Phys. Rev.* B **47** 14850
[29] Kurabayshi K 2001 *Int. J. Thermophys.* **22** 277
[30] Pietralla M 1996 *J. Comput. Aid. Des.* **3** 273
[31] Tadokoro H 1979 *Structure of Crystalline Polymers* (New York: Wiley)
[32] Avitable G, Napolitano R, Perozzi B, Rouse K D, Thomas H W and Wills B T M 1975 *J. Polym. Sci. Polym. Lett. Edn* **13** 351
[33] Choy C L, Wong Y W, Yang G W and Kanamoto T 1999 *J. Polym. Sci.* **37** 3359
[34] Kahlert H, Leitner O and Leising G 1987 *Synth. Met.* **17** 467
[35] Zhu Q, Fischer J E, Zuzok R and Roth S 1992 *Solid State Commun.* **83** 179
[36] Okamoto S and Ishida H 2001 *Macromolecules* **34** 7392
[37] Agari Y, Shimada M and Ueda A 1997 *Polymer* **38** 2649
[38] Agari Y, Ueda A, Omura Y and Nagai S 1997 *Polymer* **38** 801
[39] Dong H, Fan L and Wong C P 2005 *55th Proc. Conf. on Electronic Components and Technology* p 1451
[40] Huxtable S, Cahill D, Shenogin S, Xue L, Ozisik R, Barone P, Usrey M, Strano M S, Siddons G, Shim M and Keblinski P 2003 *Nat. Mater.* **2** 731
[41] Xue L, Keblinski P, Phillpot S R, Choi S U S and Eastman J A 2003 *J. Chem. Phys.* **118** 337
[42] Michaelson Sh, Ternyak O, Akhvlediani R, Lafosse A, Bertin M, Azria R and Hoffman A 2007 *Phys. Status Solidi* a **204** 2909
[43] Hovis J S, Coulter S K, Hamers R J, D'Evelyn M P, Russell J N Jr and Butler J E 2000 *J. Am. Chem. Soc.* **122** 732
[44] Komatsu S, Okada K, Shimizu Y and Moriyoshi Y 2001 *J. Appl. Phys.* **89** 8291
[45] Sumant A V, Grierson D S, Gerbi J E, Carlisle J A, Auciello O and Carpick R W 2007 *Phys. Rev.* B **76** 235429